Modeling and simulation of combustion in the context of rocket engine ignition

By G. Ribert, B. Duboc, U. Guven AND P. Domingo

CORIA - UMR6614 CNRS, INSA and Université de Rouen, Normandie Université
Avenue de l'université, 76800 St-Etienne-du-Rouvray, France

The goal of the present work is to provide a framework for the numerical simulation of the ignition of rocket engines. Two specific objectives were fulfiled during this summer programme. The 3D large eddy simulation of an ignitor nozzle has been successfully performed. The computational cost has been decreased by using a reduced kinetic mechanism for hydrogen-oxygen flames, validated toward a detailed mechanism. The second objective was the validation of a novel approach designed to deal with detailed chemistry, called Hybrid Transported-Tabulated Chemistry (HTTC) method, on methane and kerosene flames. A good agreement with the fully detailed chemistry results has been achieved, with a dramatic decrease of the computational cost. The impact of differential diffusion on HTTC has been investigated and a correction for the local computation of the mixture fraction has been developed.

1. Introduction

Studying the combustion in a liquid rocket engine (LRE) is a challenging task. Indeed, the ignition process and the flame anchoring occur at low-pressure. Then, the pressure inside the combustion chamber increases to a pressure level that is above the critical pressures of the reactants leading to a dramatically change in the physics of flame behaviour. Computing all these processes needs to take into consideration highly compressible turbulent flows, premixed and non-premixed flames, real gas effects, etc. The proposed work is related to the ignition phase that represents a critical operating point. The operating principle follows the classical design for LRE: oxygen and hydrogen are injected into the combustion chamber by several concentric rows of coaxial injectors. At the centre, a sonic jet of hot burnt gases starts the ignition (see Figs. 1). The correct understanding of ignition mechanisms is a major milestone in the development of the rocket upper stage as multiple re-ignitions is desired to put into orbit several satellites. The ignition of a mixture of hydrogen and oxygen by a jet of hot gases is a complex phenomenon associating turbulent mixing and finite rate chemistry effects. This problem is often studied experimentally but computations are scarce [1]. The objective of the present work is to provide a more fundamental framework for such ignition process and to assess a new strategy to handle a detailed chemistry into complex simulations. Indeed, the european rocket engine is nowadays dealing with combustion of oxygen with hydrogen, but in the context of post-Ariane 6, methane could replace hydrogen with the objectives to have a low-cost and reusable launcher.
Two specific objectives were pursued during this summer programme:

– Large eddy simulation of the ignitor nozzle, i.e. the simulation of a hot multi-species

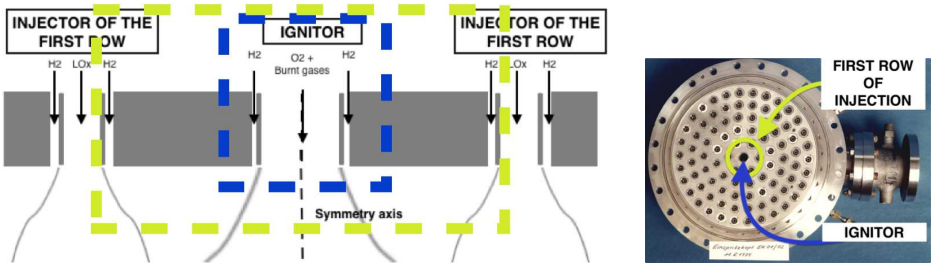

(a) (b)

FIGURE 1. Problem under study: (a) sketch of the ignitor with the first row of injection and (b) injector head.

jet coming from the combustion of oxygen-hydrogen and exiting in a low-pressure atmosphere;

– Validation of the strategy HTTC (Hybrid Transported-Tabulated Chemistry, [2]) on two extreme cases: combustion of methane and kerosene fuel.

Both studies use the finite volume code SiTCom-B which solves the unsteady compressible reacting Navier-Stokes equations on Cartesian meshes. Briefly, SiTCom-B uses fourth-order schemes for space and time discretization. The resolution of the Navier-Stokes equations is fully explicit. The boundaries are described using the three-dimensional Navier-Stokes characteristic boundary conditions (NSCBC) approach [3], ensuring minimal acoustic reflections. Further details may be found in [4] and on the dedicated website at http://www.coria-cfd.fr/index.php/SiTCom-B.

2. LES of the ignition of a rocket combustion chamber

2.1. *Problem setup*

The control of the ignition sequence in a rocket engine is a critical problem for present and future combustion chamber designs. In some cases delayed ignition may lead to a chamber pressure peak that could damage the burner. In a rocket engine the ignition is performed in four steps. First the system is purged with an inert gas (Nitrogen in our simulation) to reach a nominal state. Then hydrogen injection starts, and after a few milliseconds the igniter is triggered by injecting very lean burnt gases into the combustion chamber. Finally oxygen is injected. The purpose of the ignitor is to start the flame and the combustion between oxygen in burnt gases and hydrogen into the combustion chamber.

During this summer program, the numerical simulation of the supersonic combustion between burnt gases and hydrogen was performed. The target configuration is represented by the ignitor with the first ring of hydrogen injection. It corresponds to the green area in Fig. 1(a) and 1(b). The computational domain for the 3D-Simulation is a cylinder with the following properties: $L_x = L_y = L_z = 20$ mm. It leads to a cell size of 50 μm with a total number of cells equal to 0.17M and 85M for 2D and 3D simulations, respectively. The injection is realized at the top of the domain with the following conditions for H_2: 2 bar, 200 K, Mach 1.5; for burnt gases: 10 bar, 2000 K, Mach 1. Two kinetic schemes are used: the detailed mechanism of SAN DIEGO [5] (9 species, 21 reactions) for 2D simulations, and the reduced kinetic scheme of BOIVIN [6] (6 species, 16 reactions) for 2D and 3D simulations.

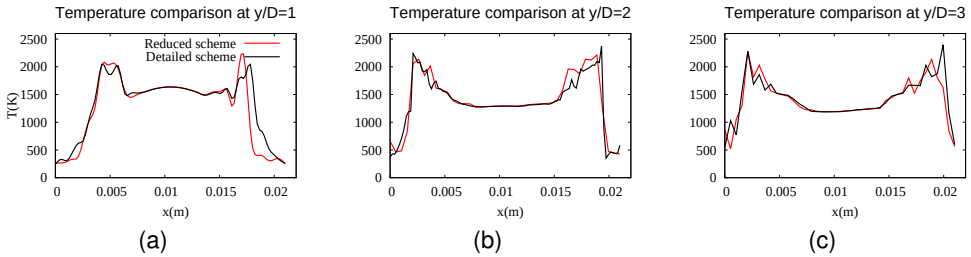

FIGURE 2. Temperature comparison.

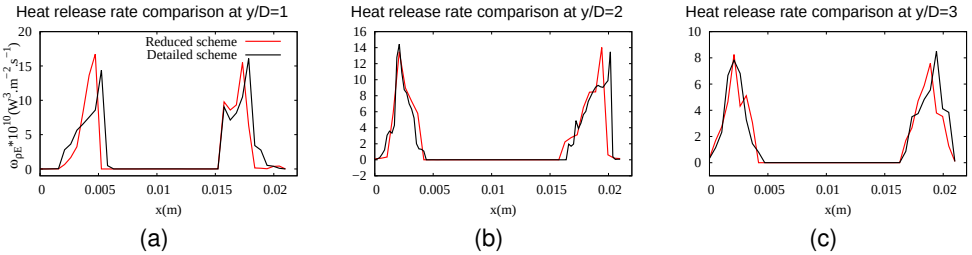

FIGURE 3. Heat release comparison.

2.2. *Simulation results*

2.2.1. *Kinetic scheme comparison*

To assess the validity of the reduced chemistry of Boivin compared to detailed chemistry, 2D simulations are performed. Initially the burner is filled with nitrogen, before the injection of hydrogen quickly followed by burnt gases. The simulation is run during two convective times (calculated from properties of burnt gases injection) in order to compute the mean values of temperature and heat release rate into the domain. The comparison between the two kinetic schemes is performed at three downstream locations y/D = 1, 2 and 3.

In Fig. 2 and Fig. 3 a similar shape is observed for the profile of temperature and heat release rate:

– Two peaks of temperature about 2000 K centered on x= 0,01 which is the center of the domain are observed. These peaks locations represent the two interfaces on a downstream location between burnt gases and hydrogen injections, which is the place where combustion mainly occurs. We also observed this behavior for the mean value of heat release rate (Fig. 3).

– The distance between the center x=0,01 and peaks locations, increases with y/D. This is mainly due to the burnt gases flow which expands (see Fig. 6).

– Between these peaks the temperature is nearly constant. $T \approx 1500$ K at y/D=1; $T \approx 1400$ K at y/D=2 and $T \approx 1300$ K at y/D=3, these decrease is mainly due to the expansion of burnt gases which imply the cooling of these gases.

– Peaks thickness also increases with y/D. Because of the temperature diffusion.

An identical behavior is then observed with both kinetic schemes, meaning that the reduced chemistry of Boivin can be used for 3D simulations. In addition, the 3D simulation with the detailed scheme was out of reach during the summer program due to its huge cost of CPU time (Tab. 1).

	Reduced scheme	Detailed scheme
Averaged time step	$4.0\ 10^{-10}s$	$2.5\ 10^{-10}s$
Time for an iteration (2D, 16 procs)	0.25 s	0.35 s
CPU costs for the simulation (2D)	55.5 h	355 h
Time for an iteration (3D, 1024 procs)	12 s	17 s
CPU costs for the simulation (3D)	170.000 h	390.000 h

TABLE 1. Performances of schemes.

2.2.2. *3D simulation*

The simulation which was performed represents the steps two and three of the ignition process. Initially the chamber is filled with nitrogen (step 1), then hydrogen is injected during a few microseconds (step 2; Fig. 4 shows the instantaneous field at this step). Once the chamber is almost filled with hydrogen burnt gases are injected (step 3). Fig. 5 shows the evolution of temperature, heat release rate, mass fraction of H (which is a product of Hydrogen/Oxygen combustion) and stoichiometric line during burnt gases injection. And Fig. 6 represents the instantaneous field after burnt gases injection.

As soon as burnt gases penetrate inside the combustion chamber, the following observations can be made:

– The pressure inside the combustion chamber being very low (0,1 bar), an under expanded flow is observed and a mach disk appears into the chamber (see Fig. 2.2.2).

– A shock wave propagates from burnt gases injection in all directions and hit the surrounding supersonic injection of hydrogen. Initially this shock is on the stoichiometric line. Then it is slowed down and it's located behind the stoichiometric line. The flame starts at first on this shock (the temperature on the shock reaches 3300K). When the stoichiometric line and the shock location are separated, the flame keep on going toward to exit and leaves the domain.

– The supersonic combustion starts instantaneously along the stoichiometric line between oxygen in burnt gases and hydrogen. At the final instant (in Fig. 6) the temperature is about 3300K along the stoichiometric line and the production of species H or H_2O are also localized along the stoichiometric line.

– A recirculation region takes place at the top of the domaine, between hydrogen injections (from the first ring and from the ignitor). On this recirculation area the axial velocity is positive.

The simulation of a rocket-like ignition configuration leads to a highly complex flow structured with shocks interaction and supersonic combustion. An under expanded flow has been identified and the combustion mainly occurs on the stoichiometric line.

Finally this 3D result shows an underexpanded flow takes place, with a lot of shocks waves. A recirculation region is also present into the burner. And the combustion starts instantaneously along the stoichiometric line, after injecting burnt gases the flame is initiated into the burner, which is the main purpose of the ignitor.

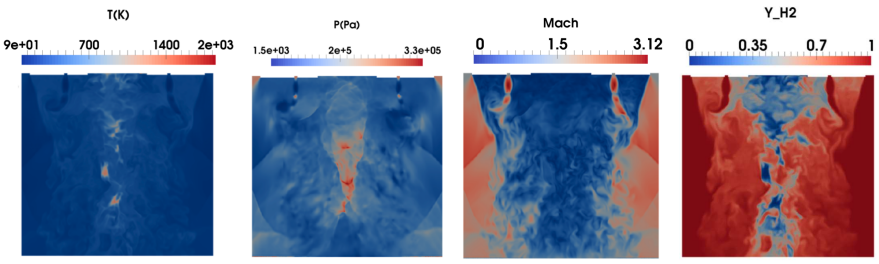

(a) Temperature (b) Pressure (c) Mach number (d) H_2 mass fraction

FIGURE 4. Instantaneous field after Hydrogen injection (step2).

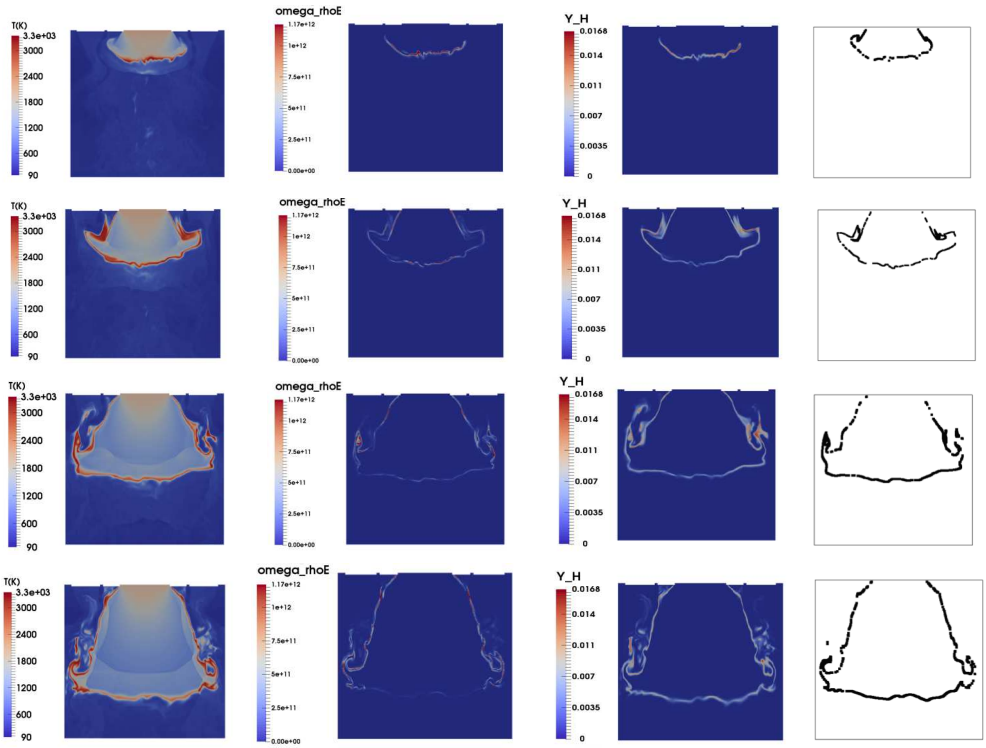

(a) Temperature (b) Heat release rate (c) H mass fraction (d) Stoichiometric line

FIGURE 5. Snapshots at different moment of instantaneous field during burnt gases injection

3. Hybrid Transported/Tabulated Chemistry

3.1. *Background and objectives*

A number of complex physical phenomena should be taken into account to properly design rocket engines. Simulating ignition process implies to introduce detailed chemistry features into the CFD codes. Indeed, simplified chemistry descriptions are able to correctly predict the burnt gases temperature and the flame speed, when the pressure and the equivalence ratio are in a given range, but generally fail when out of this range. Detailed mechanisms do not suffer from this lack of generic character and can

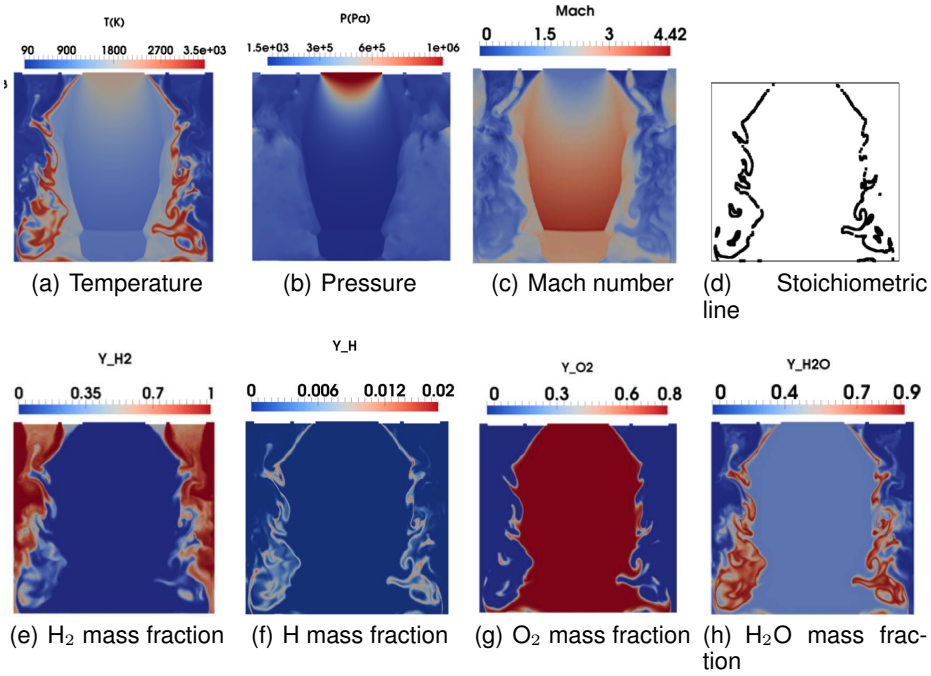

(a) Temperature (b) Pressure (c) Mach number (d) Stoichiometric line

(e) H_2 mass fraction (f) H mass fraction (g) O_2 mass fraction (h) H_2O mass fraction

FIGURE 6. Instantaneous field after burnt gases injection (step3).

offer better prediction capabilities as shown in the study detailed in the previous section. Unfortunately, LES of practical burners may be limited when using such mechanisms, because the number of transported species and reactions may be too large for today's supercomputers, especially when dealing with the combustion of hydrocarbons. For instance, for kerosene fuel, Dagaut *et al.* [7] developed a kinetic mechanism containing 225 species and 3493 reactions. For methane fuel, the mechanism of Lindstedt *et al.* [8] contains 29 species and 141 reversible reactions. A second issue appears when using a fully-explicit solver: the chemical timestep should be set to a tiny value, to properly solve the intermediate species transport equations, and is thus too small to complete a full simulation.

Solutions exist: for example, one-dimensional laminar flames can be projected into a progress variable and mixture fraction space, to build a look-up table which will be used during the simulation to extract some variables, such as the species mass fractions, instead of solving for them [9, 10]. Thus only the mixture fraction and the progress variable need to be transported with the flow, dramatically reducing the computation cost. However, the use of such tables may lead to a significant lack of accuracy and flexibility, and may become too large when the dilution by burnt gases, heat transfers or multiple inlets are considered. The size of these multidimensional tables is often considerable, which is not well-adapted to the context of high-performance computing. Hence, table downsizing methods have been discussed in the literature, using the self-similarity behavior of the radical species in laminar flamelets [11, 12].This remarkable property has been exploited by Ribert *et al.* to develop a strategy combining the detailed-chemistry solving for the main species with the tabulation of the intermediate species, called Hybrid Transported-Tabulated Chemistry (HTTC) [2]. Previously, this method has been val-

Name of the species	*Formula*	Y_k *in surrogate 1*	Y_k *in surrogate 2*
n-decane	$nC_{10}H_{22}$	1.0	0.74
n-propylbenzene	PHC_3H_7	-	0.15
n-propylcyclohexane	CYC_9H_{18}	-	0.11

TABLE 2. Composition (mass fractions) of the kerosene surrogates used in this work [15].

Surrogate 1	H_2	O_2	CO	CO_2	$nC_{10}H_{22}$	H	O
	OH	HO_2	H_2O	HCO	N_2		
Surrogate 2	H_2	O_2	CO	CO_2	$nC_{10}H_{22}$	H	O
	OH	HO_2	H_2O	HCO	N_2	PHC_3H_7	CYC_9H_{18}

TABLE 3. Tabulated species for the kerosene/air flames.

idated on one-dimensional methane/air flames, with a freely propagating flame code (REGATH [13]).

3.2. *One-dimensional kerosene/air flames*

The extreme case of combustion of kerosene is presently studied. One-dimensional flames are computed with a resolution in the flame region from 5×10^{-6} m at $P = 20$ bar to 20×10^{-6} m at $P = 1$ bar. The kinetic mechanism of Luche *et al.* [14] without NO_x (74 species and 746 non-reversible reactions) is used to model the combustion of two different kerosene surrogates (Tab. 2). The Prandtl number and the Lewis number of the flow are temperature-dependent and are computed using all the species, as well as every thermodynamic variable. The HTTC table is built for a pressure $P \in [1 \text{ bar}, 20 \text{ bar}]$, an equivalence ratio $\phi \in [0.6, 1.4]$ and a cold reactants temperature $T_u \in [500 \text{ K}, 700 \text{ K}]$, and contains 62 intermediate species mass fraction profiles. Thus only 12 species are transported for the surrogate 1 and 14 for the surrogate 2 (Tab. 3).

A good agreement between the steady fully-detailed chemistry solution from REGATH and the results obtained with SiTCom-B using HTTC is observed, for several (P, ϕ, T_u) conditions, with the surrogate 1 (pure decane). A sample of the results is shown on Fig. 7. The simulation could not have been performed using the fully-detailed chemistry solver of SiTCom-B, since the computational cost would have been prohibitive. However, the cost of the simulations with the two solvers can be compared. With HTTC the computational time is dramatically reduced (Tab. 4) by means of :

– a decrease of the wall-time per iteration, because only 12 species are transported when HTTC is used, instead of 74 for the fully-detailed chemistry.

– an increase of the chemical timestep by around 4 orders of magnitude compared with the fully-detailed chemistry, because the intermediate species are not transported anymore.

Moreover, the HTTC method is quite flexible, since it can be used with tables built on a smaller range of T_u and P than those encountered in the target application. For example, for a flame at $T_u = 500$ K, a good agreement with the fully-detailed chemistry is still achieved when using a table built at $T_u = 550$ K (Fig. 3.2). Similar results are obtained with a table fixed at $T_u = 550$ K for simulations at $T_u = 600$ K, and for simulations from 10 bar to 20 bar with a table built at $P = 15$ bar (results not shown). Good results are also

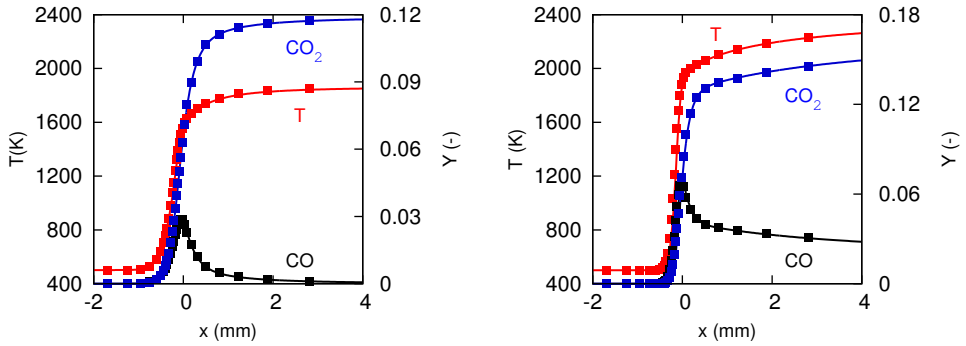

(a) $\phi = 0.6$ (b) $\phi = 1.0$

FIGURE 7. Temperature, CO and CO_2 profiles for two decane/air flames, at $P = 1$ bar and $T_u = 500$ K. Symbols : fully-detailed chemistry, lines : HTTC.

	Fully-detailed chemistry	HTTC
Wall-time per iteration (ns)	17000	11700
Chemical timestep (s)	10^{-12}	10^{-8}

TABLE 4. Computational cost for the kerosene/air simulations with SITCom-B.

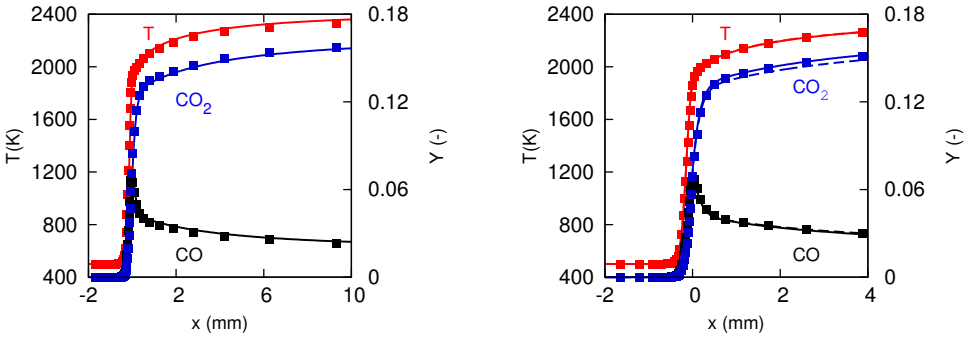

(a) Decane/air flame at $T_u = 500$ K. Symbols : fully-detailed chemistry, lines : HTTC using a table built at 550 K.

(b) Surrogate 2/air flame at $T_u = 500$ K. Symbols : fully-detailed chemistry, solid lines : HTTC with table for surrogate 2, dashed lines : HTTC with table for surrogate 1.

FIGURE 8. Temperature, CO and CO_2 profiles for kerosene/air flames, with tables built for fixed conditions.

achieved when the simulation of a surrogate 2 flame is performed, but using a table built with surrogate 1 (Fig. 3.2). Indeed, the heavy species concentrations, due to the fuel breakdown, are different for surrogates 1 and 2 (Fig. 9), because the fuel composition is different. However, similar light species concentration are obtained for both surrogates, so the product mass fractions and the heat release rate are nearly identical.

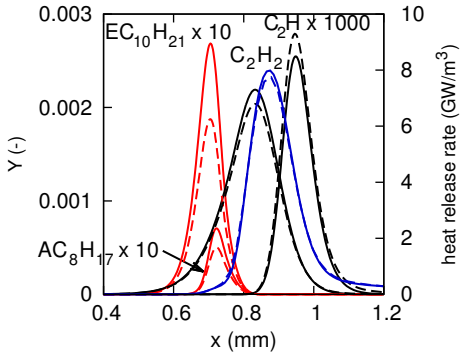

FIGURE 9. Light (black) and heavy (red) species mass fractions and heat release rate (blue) in kerosene/air flames. Solid lines : surrogate 1, dashed lines : surrogate 2.

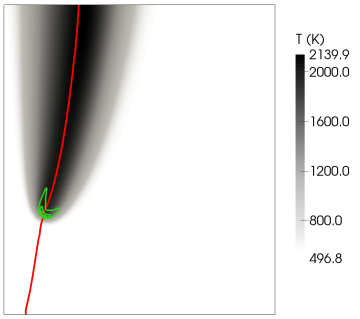

FIGURE 10. Temperature field of the computed lifted flame, with stoichiometric line (red) and heat release rate contours (green).

3.3. *HTTC efficiency for stratified combustion*

A 2D lifted methane/air flame is simulated, in order to investigate the effects of a mixture fraction gradient when using HTTC. The results are compared with a reference simulation, performed with fully-detailed chemistry.

A burner (diameter $d = 2$ mm) injects pure methane at $U_1 = 6$ m/s and $T_u = 500$ K and is surrounded by a pure air coflow at $U_2 = 2$ m/s and $T_u = 500$ K. The thickness of the burner wall is 0.5 mm. The computational domain is two-dimensional. A symmetry condition is fixed at the middle of the burner, at $x = 0$, where x is the radial axis. The kinetic mechanism of Lindstedt [8] is used. The domain length is 17.5 mm in the radial direction and 20 mm in the axial direction. The cell size is 0.05 mm in the flame zone. No subgrid model is used, because the flow is laminar and the mesh is refined enough to describe the flame front.

After the ignition, a lifted triple-flame stabilizes above the burner (Fig. 10). Results show a quite good agreement between the fully-detailed chemistry approach and HTTC (Fig. 11). The computational time is 5 times lower when using HTTC, thanks to the increase of the chemical timestep. However, some discrepancies between the two methods are observed, and they may be caused by differential diffusion effects. In this simulation, the mixture fraction Z used to access the table is not transported but reconstructed. Because of differential diffusion, Z is not constant when crossing the flame front (Fig. 12), and its local value in the flame may be different from its value in the fresh gases Z_u. In this case, the data read in the table is based on a wrong approximation of Z_u, and an error on the intermediate species is done, which affects the temperature and the product mass fractions. This phenomenon has been highlighted with a stoichiometric 1D flame (Fig. 13), where Z used to enter the table is computed locally. For each mesh point, the value of Z is either underestimated or overestimated, and the data read in the table match lean or rich flames, whereas they should match the stoichiometric flame. The consequence is an underestimated burnt gases temperature.

During this summer program, a correction has been developed in order to locally compute Z_u, to enter the table, instead of using Z given by Bilger's formula. A new variable $Y^* = Y_{\mathrm{CH_4}} \times Y_c$ is computed in each cell. Its remarkable property is that, for a given couple (Y_c, Y^*), there is a unique profile, which matches a unique value of Z_u (Fig. 14).

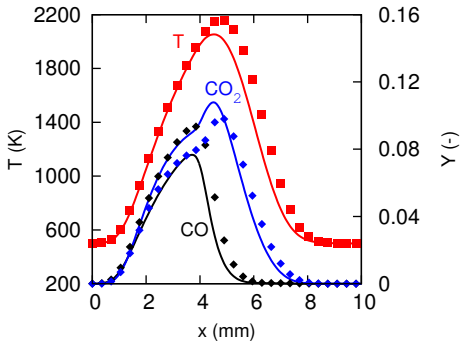

FIGURE 11. Temperature, CO and CO_2 mass fraction profiles in the lifted flame, at a height $h = 5d$ above the burner. Symbols : fully detailed chemistry, lines : HTTC.

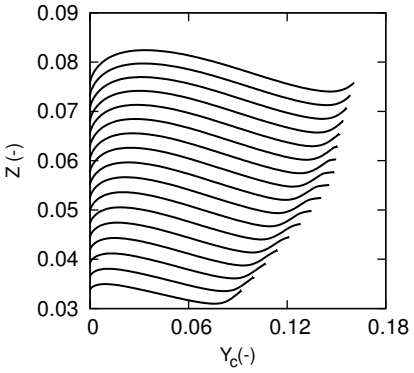

FIGURE 12. Z vs. Y_c in methane/air flames for different values of $Z_u \in [0.0338, 0, 0754]$ (i.e $\phi_u \in [0.6, 1.4]$).

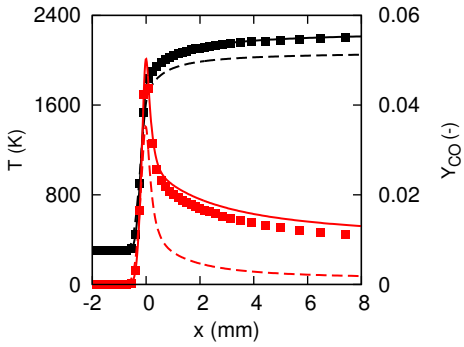

FIGURE 13. Temperature and CO mass fraction profiles in a stoichiometric methane/air flame. Symbols : fully-detailed chemistry, dashed lines : HTTC with Z computed locally with no correction, solid line : HTTC with a corrected Z computed locally.

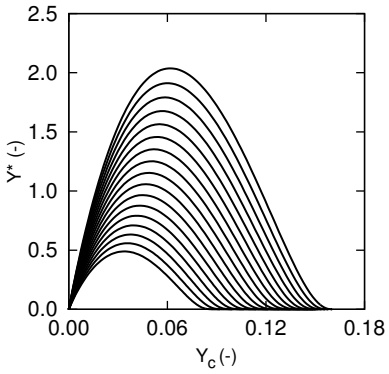

FIGURE 14. Y^* vs. Y_c in methane/air flames for different values of $Z_u \in [0.0338, 0, 0754]$ (i.e $\phi_u \in [0.6, 1.4]$).

It should be noted that in the fresh gases, $Y_c = 0$, and then $Y^* = 0, \ \forall Z_u$. Nevertheless no correction is needed in the fresh gases because here $Z = Z_u$. Hence, the array $Z_u(Y_c, Y^*, P, T_u)$ can be stored in the table. Once the value of Z_u has been fetched, the intermediate species mass fractions are read in the table.

4. Conclusion

Two specific objectives were pursued during this summer programme.
The first one was to simulate a rocket-like ignitor. A comparison between reduced and detailed scheme was performed. Results show a good agreement between both kinetic schemes. The reduced mechanism was used for 3D simulation because it costs cheaper in CPU time than the detailed scheme. Then the 3D simulation of the supersonic combustion between lean burnt gases and hydrogen was performed with LES method (85 M of cells). Results show that combustion starts instantaneously along the stoichiometric

line. This database will be further analyzed to characterize the regime of combustion. A refine simulation will be performed to assess the influence of the mesh resolution in the ignitor behavior.
The second objective was the validation of the HTTC approach, on the combustion of methane and kerosene. A good agreement with the fully-detailed chemistry results has been obtained, on both 1D and 2D cases, with methane and kerosene. The computational cost has been reduced by several orders of magnitude, by dramatically increasing the chemical timestep and by reducing the wall-time per time iteration. A method to locally correct the value of the mixture fraction, in order to get the value corresponding to the fresh mixture, has been developed and validated on 1D flames. In a future work, this method will be tested on the lifted flame.

Acknowledgments

Financial support has been provided by the German Research Foundation (Deutsche Forschungsgemeinschaft – DFG) in the framework of the Sonderforschungsbereich Transregio 40. Computations have been performed using HPC resources from CRIHAN and GENCI (CCRT/CINES/IDRIS).

References

[1] BOUHERAOUA, L. (2014). Modelisation and Simulation of the supersonic combustion. *PhD thesis*,CORIA - ROUEN

[2] RIBERT, G., VERVISCH, L., DOMINGO, P., AND NIU, Y.-S. (2014). Hybrid Transported-Tabulated Strategy to downsize detailed chemistry for numerical simulation of premixed flames. *Flow Turbulence Combust.*, **92**, 175–200.

[3] LODATO, G., VERVISCH, L. AND DOMINGO P. (2008). Three-dimensional boundary conditions for direct and large-eddy simulation of compressible viscous flows. *J. Comput. Phys.*, **227**, 5105–5143.

[4] PETIT, X., RIBERT, G, DOMINGO, P. AND LARTIGUE, G. (2013). Large-eddy simulation of supercritical fluid injection. *J. Supercritical Fluids*, **84**, 61–73.

[5] WILLIAMS, F.A. (2010). Chemical-Kinetic mechanisms for combustion applications. San Diego - University of California.

[6] BOIVIN, P. (2011). A four-step reduced mechanism for syngas combustion. *Combustion and Flame.*, **158**, 1059–1063.

[7] DAGAUT, P., REUILLON, M., CATHONNET, M. AND VOISIN, D. (1995). High pressure oxidation of normal decane and kerosene in dilute conditions from low to high temperature. *J. Chim. Phys.*, **92**, 47–76.

[8] LINDSTEDT, P. (1998). Modeling of the chemical complexities of flames. *Symposium (International) on Combustion*, **27**(1), 269–285.

[9] LODIER, G., VERVISCH, L., MOUREAU, V. AND DOMINGO, P. (2011). Composition-space premixed flamelet solution with differential diffusion for in situ flamelet-generated manifolds. *Combustion and flame*, **158**(10), 2009–2016.

[10] NGUYEN, P.-D., VERVISCH, L., SUBRAMANIAN, V. AND DOMINGO, P. (2010). Multidimensional flamelet-generated manifolds for partially premixed combustion. *Combustion and flame*, **157**(1), 43–61.

[11] RIBERT, G., GICQUEL, O., DARABIHA, N. AND VEYNANTE, D. (2006). Tabulation of complex chemistry based on self-similar behavior of laminar premixed flames. *Combustion and flame*, **146**(4), 649–664.

[12] RIBERT, G., WANG, K. AND VERVISCH, L. (2010). A multi-zone self-similar chemistry tabulation with application to auto-ignition including cool-flames effects. *Fuel*, **91**(1), 87–92.

[13] DARABIHA, N. (1992). Transient behaviour of laminar counterflow hydrogen-air diffusion flames with complex chemistry. *Combustion Science and Technology*, **86**(1-6), 163–181.

[14] LUCHE, J., REUILLON, M., BOETTNER, J.-C. AND CATHONNET, M. (2004). Reduction of large detailed kinetic mechanisms: application to kerosene/air combustion. *Combustion Science and Technology*, **176**(11), 1935–1963.

[15] GUÉRET, C., CATHONNET, M., BOETTNER, J.-C AND GAILLARD F. (1991). Experimental study and modeling of kerosene oxidation in a jet-stirred flow reactor. *Symposium (International) on Combustion*, **23**(1), 211–216.

[16] ZELDOVICH, Y. (1946). *Acta Physicochim.*

[17] MALTE, P. C. AND PRATT, D. T. (1974). The role of energy-releasing kinetics in NOx formation: fuel-lean, jet-stirred CO-air combustion. *Combustion Science and Technology*, **9**(5-6), 221–231.

[18] MILLER, J.-A. AND BOWMAN, C.-T. (1989). Mechanism and modeling of nitrogen chemistry in combustion. *Prog. Energy Combust. Sci.*, **15**(4), 287–338.

[19] http://www.me.berkeley.edu/gri_mech/

[20] BILGER, R. W., STARNER, S. H. AND KEE, R. J. (1990). On reduced mechanisms for methane-air combustion in nonpremixed flames. *Combustion and flame*, **80**(2), 135–149.